IABSE-JSCE Joint Conference on Advances in Bridge Engineering-II, August 8-10, 2010, Dhaka, Bangladesh. ISBN: 978-984-33-1893-0
Amin, Okui, Bhuiyan (eds.) www.iabse-bd.org

# The lateral strength and ductility of the piers of Khilgaon Flyover in Dhaka

M.A. Kader & M.M. Hoque
*Department of Civil Engineering, Dhaka University and Engineering and Technology, Gazipur, Bangladesh*

ABSTRACT: Lateral strengths of the piers of Khilgaon flyover have been evaluated analytically under bending, and shear mode of failure independently. The lateral strengths in bending are obtained using the results of nonlinear sectional analyses of the pier sections, while the shear strength of the piers are calculated using code defined equation taking into account the effect of depth, volumetric ratio of lateral steel, crushing strength of concrete, yield strength of steel. A fiber model of the pier sections at the critical positions are developed for obtaining $M-\phi$ relationships. Subsequently, nonlinear pushover analyses of the piers are carried out to obtain $P-\Delta$ relationships. The material nonlinearity is taken into accounted for sectional analysis, while the material and geometric nonlinearity are considered for pushover analyses. In this study, ultimate capacities in bending and shear, yield and ultimate displacement, ultimate and allowable ductility are obtained from $M-\phi$ and $P-\Delta$ relationships. Ductility are expressed in terms of both curvature and displacement ductility. Finally, the lateral strengths of the piers are presented in normalized form.

## 1 INTRODUCTION

Fly-overs are lifeline structures that play a vital role in the surface mode of transportation. In the case of natural disaster, the fly-overs play a very important role for evacuation, and offer emergency route for rescue, first aid, medical services firefighting, and transporting relief goods to the refugees as well. However, the fly-overs are potentially one of the most vulnerable structures in a highway system. Thus the risk, reliability and safety of a highway system largely depends on the safety of the fly-overs. Flyovers are being constructed to reduce a remarkable traffic congestion of mega city, Dhaka. Two flyovers namely Mohakhali flyover and Khilgaon flyover have already been constructed in Bangladesh, and many of them are in the queue. Khilgaon is the second one according construction sequence. Alike other bridges, the fly-overs are designed o the basis strength criteria under gravity loads, lateral loads. Among different lateral loads, earthquake and wind loads govern the design criteria of lateral loads.

Bangladesh lies within a seismically active region. Due to existence of active faults, there is a high probability of occurrence of moderate to large magnitude earthquakes (Ali and Choudhury, 1994; 1992). Hence, it is necessary to predict the probable losses due to future earthquakes, to assess the seismic safety, plan for seismic retrofitting, pre-earthquake and disaster mitigating plan. One of the ways to assess probable losses under an earthquake required is to investigate the seismic vulnerability of structures. Seismic vulnerability can be assessed in two ways: empirically and analytically. Empirical vulnerability analyses are virtually impossible for Bangladesh, since structural damage data due to earthquakes are not available. Hence, analytical vulnerability analysis is the only choice to be made for obtaining vulnerability of structures.

Seismic safety concepts in earthquake resistant design philosophy all over the world can be summarized as follows: structures shall resist earthquakes of small to moderate magnitudes without damage; large magnitude earthquake excitations may lead to damage but should ensure reparability and no collapse condition of the structures. To achieve this goals, seismic codes (JRA, 2002; JSCE, 2000; CalTrans, 1999; Euro Code, 1998; ASHTO, 1998) uses the concepts of no damage under moderate earthquakes, admissible damages are restricted for large magnitude earthquakes. More elaborately, structures are allowed to behave nonlinearly and undergo certain deformations as well as energy dissipation for minimizing the losses and ensuring economy. The seismic vulnerability of flyovers due to an earthquake depends on the lateral strength-deformation characteristics and seismic response of structure. Lateral strengths and deformation characteristics of structures are to obtain for carrying out analytical vulnerability of structures.

On the basis of the background, the study aims at obtaining the lateral strength and deformation characteristics of the piers by carrying out nonlinear analyses. The lateral strengths of pier depend on the bending and shear strength of pier. The lateral strengths of the piers are obtained bending and the shear capacity. The bending strengths are obtained from sectional analysis results, while the shear strengths are estimated by using code defined equations. The bending deformations are normalized in the form of curvature ductility. The overall deformation of the pier is obtained from pushover analyses. The ultimate and allowable ductility are also evaluated based on the analytical results obtained from both sectional analysis and pushover analysis.

### 1.1 *Brief description of Khilgaon Flyover and the piers*

Khilgaon flyover has three arms namely Malibagh, Rajarbagh, Sayedabad and one loop Malibagh. The flyover is 1.9 km long, 14 wide for arms and 7 wide for loops. The span lengths are 16.0 meters to 28 meters. The piers sections are circular 1.5m and 2.0m diameter with hammerhead. The heights of the piers above the pile cap are 6.35 meters to 11.72 meters. The elevation and cross-section of a typical pier is shown in Figure 1. The piers heights above the pile cap vary from. The height, sectional dimensions, longitudinal reinforcement, transverse reinforcement is presented in tabular form in Table1.

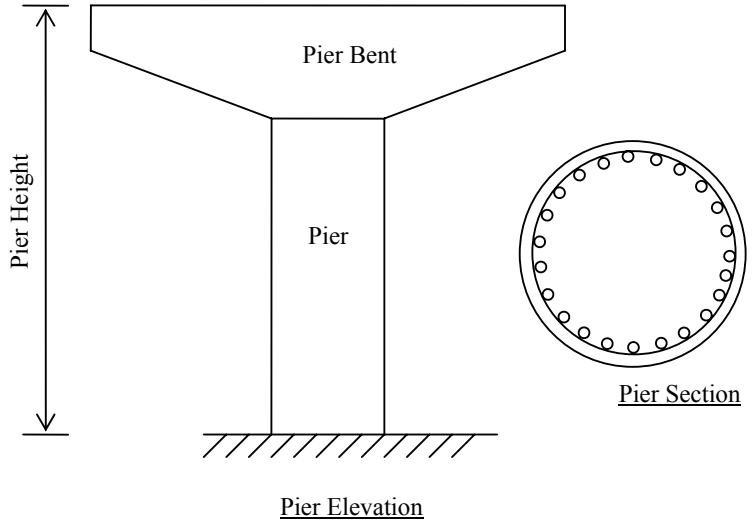


Figure 1. Elevation and Cross-section of a typical pier of Khilgaon flyover

Table-1: Piers of Khilgaon flyover

| Pier ID | Pier height (m) | Diameter (m) | Longitudinal reinforcing steel ratio (%) | Volumetric ratio of transverse steel (%) |
|---|---|---|---|---|
| PML03 to PML05 | 6.844 to 8.658 | 1.5 | 1.61 | 0.30 |
| PML06 to PML08 and PML13 | 9.650 to11.081 | 1.5 | 2.64 | 0.30 |
| PML11, PML12, PML14 | 11.723 to 11.276 | 1.5 | 2.82 | 0.30 |
| PML15, PML16 | 9.731, 8.732 | 1.5 | 2.28 | 0.30 |
| PR02 to PR12 | 7.888 | 2.0 | 0.91 | 0.22 |
| PR03 to PR12 | 6.386 to 7.338 | 2.0 | 0.91 | 0.22 |
| PS02 to PS10 | 7.292 to 7.424 | 2.0 | 0.91 | 0.22 |
| PM02 to PM07 | 6.351 to 7.286 | 2.0 | 0.91 | 0.22 |

## 2 MATERIALS AND METHODS

### 2.1 *Materials properties*

The strengths and ductility of the piers largely depend on the material strengths and stress-strain relationship. Material strengths are found from the design data. The design strengths are: for pier $f_c^{'} = 25$ MPa; yield strength of reinforcing steel, $f_y = 60$ ksi. The modulus of elasticity of concrete is $E_C = 23600$ MPa and reinforcing steel is 200000 MPa.

## 2.2 *Constitutive model of materials*

Constitutive model of the materials i.e., stress-strain relationship play the vital role of the piers analyses results. The moment-curvature relationship of particular section may vary for the different constitutive model of reinforcing steel and concrete. For this reason, a perfect model for stress-strain relationship of the materials has been a great challenge over the years. In the early days, the constitutive model for unconfined concrete (Wang at al., 1987; Ahmad and Shah, 1982) had been used. The effect of confinement of concrete

With the advancement of experimental facilities, along with experimental investigation, the effect of is now available in literatures (Mander at al., 1988a, 1988b, Hoshikuma et al., 1997). One such model, which has been used extensively in recent years, was developed by Hoshikuma et al. (1997). The descending branch of the material law as well as the increase of strength and corresponding strain because of a confining reinforcement is taken into consideration which is shown in Figure 2. The authors provided some insight into the behavior of tied columns under axial and flexural loading. The model stress-strain curve consist the three parts i.e., an ascending branch, falling branch, and sustaining branch. The graphical presentation of the Hoshikuma et al. (1997) model is given as below:

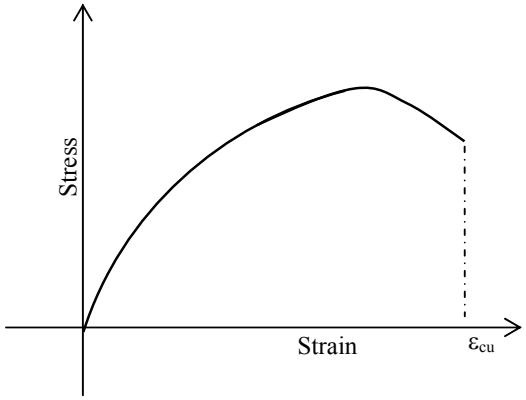


Figure 2. Constitutive model of concrete

The elastic perfectly plastic model for reinforcing steel is used in the study. The yield strength is taken as the design yield strength used in the design. The modulus of elasticity of reinforcing steel considered in the study is $2\times10^5$ MPa. The ultimate strain used is 0.01 mm/mm. A constitutive model of reinforcing steel is shown in Figure 3.

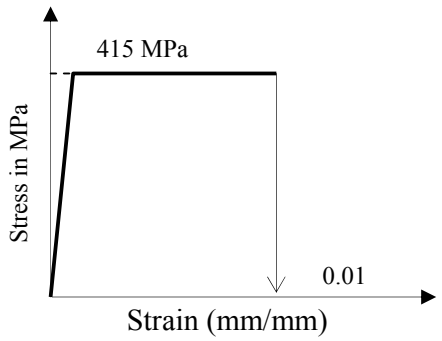


Figure 3. constitutive model of reinforcing steel

## 2.3 *Fiber model*

In sectional analysis, the mechanical behavior of a section is analyzed in fiber model using the constitutive relationships of the material, and taking the equilibrium and kinematics into considerations. The fiber model is based on the assumptions that the deformed sections remain plain, the shear deformations are not taken into account; constitutive model of materials are known. In preparing the fiber model, the reinforced concrete cross-section is divided into a number of discrete fibers. The number of fibers is taken around fifty which is

recommended by design specifications (JRA, 2002). First of all, a number of extreme compressive strains starting from small value to ultimate compressive strain are assumed. For the assumed extreme compressive strains, the depth of neutral axis is determined from the equilibrium of axial force. Having computed the strain of each fiber for a particular extreme strain, the corresponding stresses are determined using the constitutive model of the material. Integration of the stresses gives the resulting internal forces. The moment capacity corresponding to each neutral axis depth is then plotted versus the curvature. The process can continue until the ultimate compressive strain of concrete.

### 2.4 *Pushover Analysis*

To obtain the force-displacement relationship at the top of the bridge pier, the pier is divided into N slices (50 slices are recommended in the code) along its height. For sectional analysis, it is mainly focused on three sections: 1) section at the top level, 2) section at one-third level from the bottom of the pier, and 3) section at the base level. This is because the configuration of the reinforcement at this level is different. Finally, the force displacement relationship at the top of the bridge pier is obtained using the moment-curvature diagrams and shear stress-strain diagram. Figure 4 shows the numerical evaluation of the flexural and shear components of displacement. The steps for obtaining the force-displacement relationships are as follows:

1. The pier is divided into N slices along its height
2. The moment-curvature diagrams for each cross-section is obtained through sectional analysis
3. The horizontal force P is applied at the top of the pier
4. The bending moment diagrams of the pier for the applied force P is drawn
5. The curvature from bending moment and moment-curvature diagram is obtained
6. The displacement δ at the top of the pier is estimated using the following equation:

$$\delta = \sum_{i=1}^{N} \phi_i \times dy \times d_i \tag{4.1}$$

7. In a similar way, several forces P are applied and the corresponding displacement obtain. Finally, using these values, the force –displacement relationship at pier top is obtained.

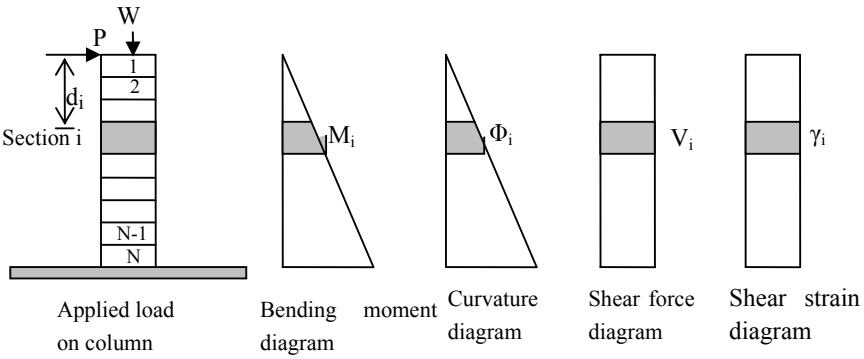


Figure 4. Numerical evaluation of flexural and shear component of displacement

### 2.5 *Lateral strength*

Lateral strengths of the piers in bending are obtained by using the ultimate moment capacities of the pier obtained from sectional analysis. The lateral strengths in flexure are found from Eq 2.2

$$P_u = \frac{M_u}{H_P} \tag{2.2}$$

where $P_u$ =ultimate lateral strength in bending, $M_u$ =ultimate moment capacity of the pier section obtained from Sectional analysis, $H_P$ = height of the pier.

The lateral strength of the piers in shear are estimated from the code JRA Standard Specifications (2002) and the AASHTO Standard Specifications (2002) adapted equations. The JRA standard specification, shear strength in a pier is resisted by concrete and shear reinforcements. The shear strengths of the piers are calculated by the JRA code adapted equations 2.3 to 2.5

$$V = V_c + V_s \tag{2.3}$$

$$V_c = c_c c_e c_{pt} f_c' bd \tag{2.4}$$

$$V_s = \frac{A_w f_{sy} (\sin\theta + \cos\theta)}{s} \tag{2.5}$$

where
where
$V$ : Shear strength (N)
$V_c$ : Shear strength resisted by concrete (N)
$V_s$ : Shear strength borne by hoop ties (N).
$f_c'$ : Average shear stress that can be borne by concrete (N/mm$^2$).
$c_c$ : Modification factor on the effects of alternating cyclic loading .Cc shall be taken as 0.6 for type 1 earthquake ground motion and 0.8 for Type-II.
$c_e$ : Modification factor in relation to the effective height (d) of a pier section
$c_{pt}$ : Modification factor in relation to the axial tensile reinforcement ratio $\rho_t$ .
$b$ : Width of a pier section perpendicular to the direction in calculating shear strength (mm).
$d$ : Effective height of a pier section parallel to the direction in calculating shear strength (mm).
$\rho_t$ : Axial tensile reinforcement ratio.
$A_w$ : Sectional area of hoop type arranged with and interval of $\alpha$ and angle (mm$^2$)
$f_{sy}$ : Yield point of hoop ties (N/mm$^2$)
$\theta$ : Angle formed between hoop ties and the vertical axis (degree)
$s$ : Spacing of hoop ties (mm)

The AASHOTO Standard Specifications (2002) adapted the following equations based on 45 degree truss model in determination of the nominal shear strength of reinforcement concrete columns.

$$V_n = V_c + V_s \tag{2.3}$$

$$V_c = \left(\frac{10P}{f_c' A_g}\right)\frac{\sqrt{f_c'}}{6} bd \tag{2.4}$$

$$V_s = \frac{A_w f_{sy} d}{s} \tag{2.5}$$

In the case of AASHTO, the effect of many parameters has not been accounted for as done in JRA equations.

## 2.6 *Ductility evaluation*

Ductility is of two types: curvature ductility and displacement ductility. Displacement ductility can be related to curvature ductility. In the study, curvature and displacement ductility are estimated. Ductility capacity of a reinforced concrete column shall be calculated depending of the failure mode as follows: Ductility capacity for flexural failure shall be calculated by equation (2.13)

$$\mu_c = 1 + \frac{\phi_u - \phi_y}{\alpha\phi_y} \tag{2.13}$$

$$\mu_d = 1 + \frac{\delta_u - \delta_y}{\alpha\delta_y} \tag{2.13}$$

where
$\mu_c$ : Curvature ductility capacity of the reinforced concrete column
$\mu_d$ : Displacement ductility capacity of the reinforced concrete column
$\phi_u$ : Ultimate curvature of the reinforced concrete column
$\phi_y$ : Yield curvature of the reinforced concrete column
$\delta_u$ : Ultimate displacement of the reinforced concrete column
$\delta_y$ : Yield displacement of the reinforced concrete column
$\alpha$ : Safety factor, 1.5 for near field and 3.0 for far field earthquake.

## 3 RESULTS AND DISCUSSION

The study was aimed at evaluating the lateral strength, ultimate and allowable ductility of the piers of Khilgaon flyover piers. As mentioned earlier, the lateral load carrying capacities are obtained in terms of bending and shear strengths. In order to achieve the goal, nonlinear sectional analysis of the piers sections, pushover analysis are carried out for the piers. $M-\phi$ relationships are obtained from the nonlinear sectional analysis and $P-\Delta$ relationships are obtained from pushover analysis, and the respective results are presented at first step, and the lateral strength-deformations are obtained and presented in the subsequent steps. As stated earlier and presented in Table 1, different cross-section and different pier types have been used, the $M-\phi$ and $P-\Delta$ relations are obtained for all the pier sections, and presented in the subsequent sections.

### 3.1 *Moment-curvature relationship*

The moment-curvature relationships are obtained using the sectional analysis of the piers. The moment-curvature relationships of the piers are graphically presented in Figure 5.

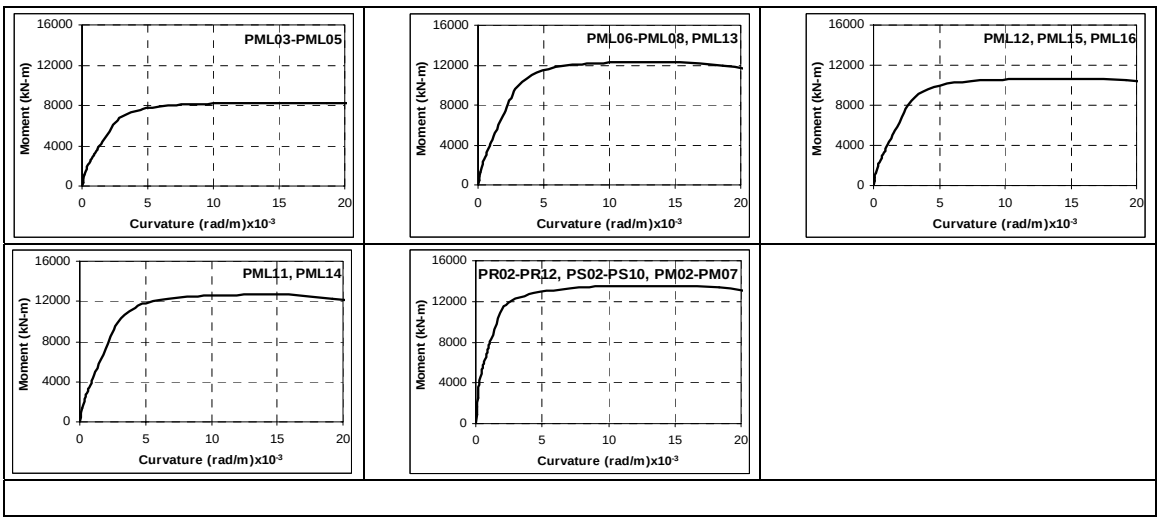


Figure 5. Moment-curvature relationship of the pier bottom sections

It is seen from Figure 5 that the moment is found to increase rapidly with increasing curvatures initially, while the rate of increase becomes insignificant after an interval. The reason for changing the relation is that reinforcing steel in the extreme tensile layer reaches yield strength. The moment in the stage is termed as yield moment. Moments are observed to increase further with curvature beyond the yield moment due to the fact that the reinforcement in layers other than in extreme layers is yet to reach yield strength. . Further, a minor change in the slope is observed in the initial linear regime. It is due to developing tension cracks in the cover concrete, and hence reduction of effective cross-sectional area occurs. It is also seen that the trend of moment-curvature relationships are for the section same but the slopes, and the characteristic points are found different for different pier cross-sections. The characteristic moment are termed as yield moment and ultimate moment.

It is found from the figures that the moment curvature relation changes with the change in diameter of the pier. For piers of particular diameter, the yield and ultimate moment increase with the increase of longitudinal reinforcement of the pier. Moreover, the slope of the initial regime increases with the increase of longitudinal reinforcement. Very large stiffness can be seen for pier of larger diameter.

### 3.2 *Load-displacement relationship*

With a view to achieve the goal, inelastic pushover analyses are carried out for obtaining the $P-\Delta$ relations. The pushover analysis results for the piers are presented in the form of load-displacement relationships that are presented in Figure 6.

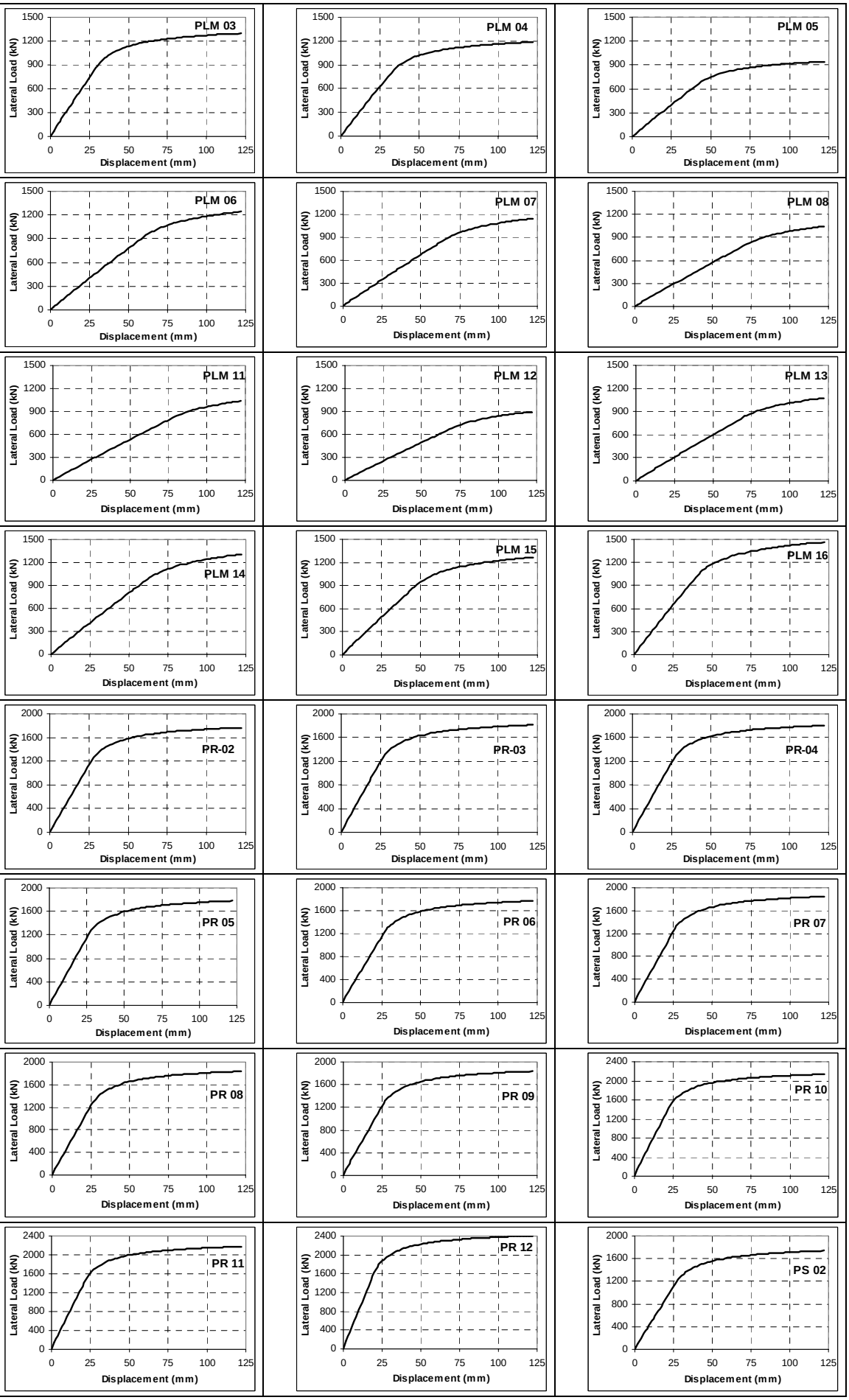
PLM 03
PLM 04
PLM 05
PLM 06
PLM 07
PLM 08
PLM 11
PLM 12
PLM 13
PLM 14
PLM 15
PLM 16
PR-02
PR-03
PR-04
PR 05
PR 06
PR 07
PR 08
PR 09
PR 10
PR 11
PR 12
PS 02
Lateral Load (kN)
Displacement (mm)

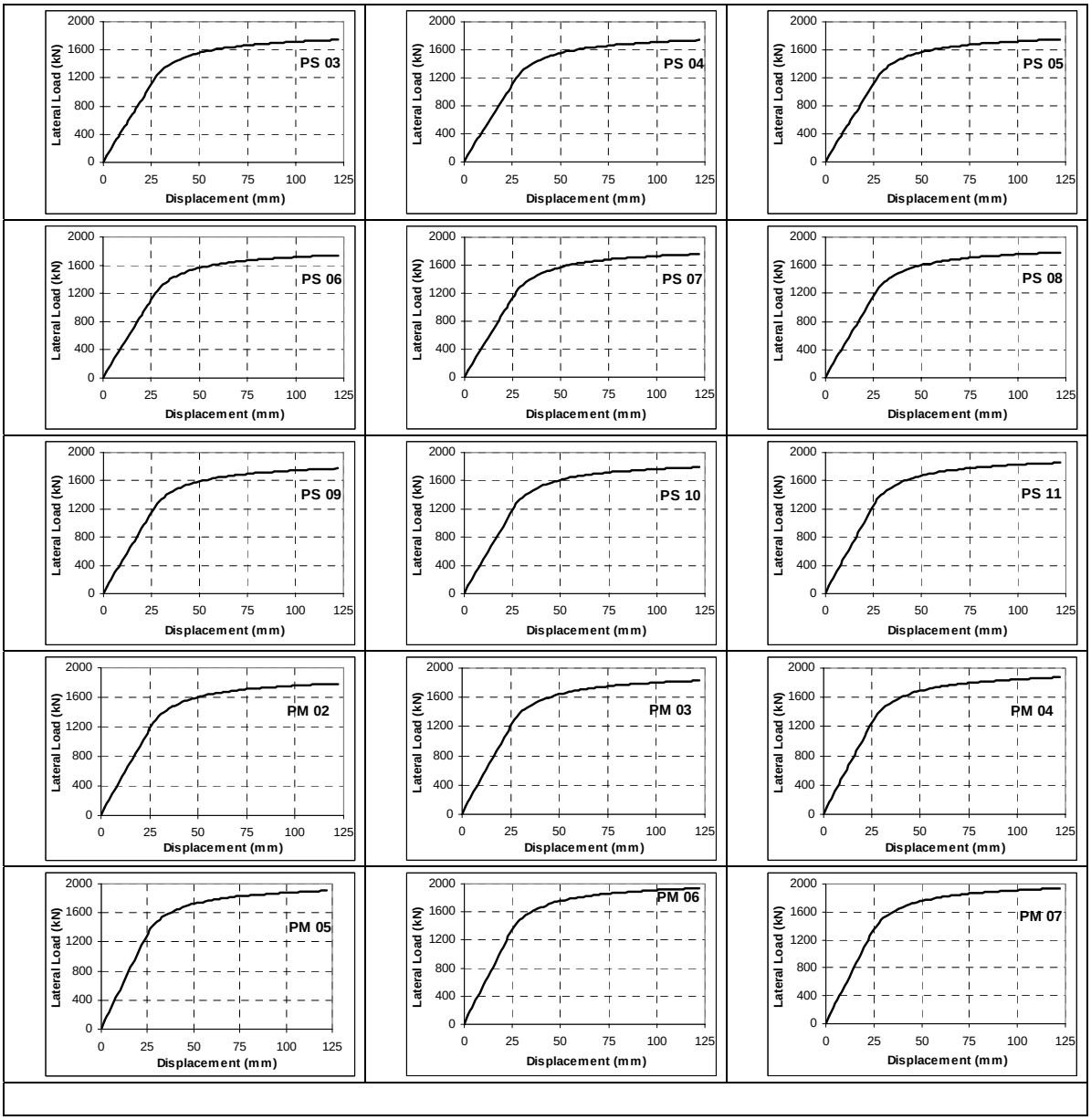

Figure 6. Load-displacement relationship of the piers

A trend similar to moment-curvature relationship has been observed in the load-displacement relationship. The reason can also been explained in similar way. From the figures, the yield and ultimate lateral load that can be carried by the piers are obtained. In addition, the yield and ultimate displacements are used in the evaluation of piers' ductility.

### 3.3 *Ductility*

The curvature and displacement ductility of the piers are estimated from the curvature and displacement of the piers on the basis of assumption that the piers will fail in bending mode. The curvature and displacement ductility of the piers is presented in tabular form in Table 2 and Table 3. The allowable ductility presented in Table 2 and Table 3 are only for far field earthquakes.

Table 2: The yield and ultimate curvature, ultimate and allowable curvature ductility of Khilgaon flyover piers.

| Pier ID | Yield curvature (1/km) | Ultimate curvature (1/km) | Ultimate curvature ductility | *Allowable curvature ductility | Allowable curvature ductility |
|---|---|---|---|---|---|
| PML03 | 2.50 | 10.50 | 4.20 | 3.13 | 2.07 |
| PML04 | 2.52 | 10.50 | 4.17 | 3.11 | 2.06 |
| PML05 | 2.52 | 10.50 | 4.17 | 3.11 | 2.06 |
| PML06 | 2.77 | 12.71 | 4.59 | 3.39 | 2.20 |
| PML07 | 2.72 | 12.72 | 4.68 | 3.45 | 2.23 |
| PML08 | 2.77 | 13.98 | 5.05 | 3.70 | 2.35 |
| PML11 | 2.85 | 13.10 | 4.60 | 3.40 | 2.20 |
| PML12 | 2.85 | 11.92 | 4.18 | 3.12 | 2.06 |
| PML13 | 2.77 | 12.72 | 4.59 | 3.39 | 2.20 |
| PML14 | 2.85 | 13.10 | 4.60 | 3.40 | 2.20 |
| PML15 | 2.6 | 11.92 | 4.58 | 3.39 | 2.19 |
| PML16 | 2.52 | 10.50 | 4.17 | 3.11 | 2.06 |
| PR02 | 1.86 | 7.20 | 3.87 | 2.91 | 1.96 |
| PR03 | 1.86 | 7.10 | 3.82 | 2.88 | 1.94 |
| PR04 | 1.86 | 7.10 | 3.82 | 2.88 | 1.94 |
| PR05 | 1.86 | 7.10 | 3.82 | 2.88 | 1.94 |
| PR06 | 1.86 | 7.10 | 3.82 | 2.88 | 1.94 |
| PR07 | 1.86 | 7.10 | 3.82 | 2.88 | 1.94 |
| PR08 | 1.86 | 7.10 | 3.82 | 2.88 | 1.94 |
| PR09 | 1.86 | 7.10 | 3.82 | 2.88 | 1.94 |
| PR10 | 1.86 | 7.10 | 3.82 | 2.88 | 1.94 |
| PR11 | 1.86 | 7.20 | 3.87 | 2.91 | 1.96 |
| PR12 | 1.86 | 6.42 | 3.45 | 2.63 | 1.82 |
| PS02 | 1.86 | 7.10 | 3.82 | 2.88 | 1.94 |
| PS03 | 1.86 | 7.10 | 3.82 | 2.88 | 1.94 |
| PS04 | 1.86 | 7.10 | 3.82 | 2.88 | 1.94 |
| PS05 | 1.86 | 7.20 | 3.87 | 2.91 | 1.96 |
| PS06 | 1.86 | 7.20 | 3.87 | 2.91 | 1.96 |
| PS07 | 1.86 | 7.20 | 3.87 | 2.91 | 1.96 |
| PS08 | 1.86 | 7.20 | 3.87 | 2.91 | 1.96 |
| PS09 | 1.86 | 7.20 | 3.87 | 2.91 | 1.96 |
| PS10 | 1.86 | 7.20 | 3.87 | 2.91 | 1.96 |
| PM02 | 1.86 | 7.10 | 3.82 | 2.88 | 1.94 |
| PM03 | 1.86 | 7.10 | 3.82 | 2.88 | 1.94 |
| PM04 | 1.86 | 7.10 | 3.82 | 2.88 | 1.94 |
| PM05 | 1.86 | 7.10 | 3.82 | 2.88 | 1.94 |
| PM06 | 1.86 | 7.10 | 3.82 | 2.88 | 1.94 |
| PM07 | 1.86 | 7.10 | 3.82 | 2.88 | 1.94 |

Note: * allowable ductility has been calculated considering far field earthquake

Table 3: The yield and ultimate displacement, ultimate and allowable displacement ductility of Khilgaon flyover piers.

| Pier ID | Ultimate load (kN) | Yield displacement (mm) | Ultimate displacement (mm) | Ultimate displacement ductility | *Allowable displacement ductility | Allowable displacement ductility |
|---|---|---|---|---|---|---|
| PML03 | 1185 | 52.5 | 91.3 | 1.74 | 1.49 | 1.25 |
| PML04 | 1142 | 60.6 | 102.2 | 1.69 | 1.46 | 1.23 |
| PML05 | 972 | 63.5 | 113.1 | 1.78 | 1.52 | 1.26 |
| PML06 | 1254 | 87.4 | 156.5 | 1.79 | 1.53 | 1.26 |
| PML07 | 1195 | 96.0 | 169.8 | 1.77 | 1.51 | 1.26 |
| PML08 | 1178 | 106.0 | 194.0 | 1.83 | 1.55 | 1.28 |
| PML11 | 1134 | 114.0 | 201.3 | 1.77 | 1.51 | 1.26 |
| PML12 | 965 | 105.0 | 177.8 | 1.69 | 1.46 | 1.23 |
| PML13 | 1133 | 102.0 | 178.7 | 1.75 | 1.50 | 1.25 |
| PML14 | 1093 | 89.9 | 161.8 | 1.80 | 1.53 | 1.27 |
| PML15 | 1218 | 69.8 | 128.2 | 1.84 | 1.56 | 1.28 |
| PML16 | 1051 | 59.7 | 104.7 | 1.75 | 1.50 | 1.25 |
| PR02 | 1862 | 41.3 | 77.8 | 1.88 | 1.59 | 1.29 |
| PR03 | 1857 | 40.5 | 75.6 | 1.87 | 1.58 | 1.29 |
| PR04 | 1851 | 40.6 | 75.9 | 1.87 | 1.58 | 1.29 |
| PR05 | 1834 | 40.9 | 76.5 | 1.87 | 1.58 | 1.29 |
| PR06 | 1827 | 41.0 | 76.8 | 1.87 | 1.58 | 1.29 |
| PR07 | 1880 | 39.0 | 73.7 | 1.89 | 1.59 | 1.30 |
| PR08 | 1880 | 39.1 | 73.9 | 1.89 | 1.59 | 1.30 |
| PR09 | 1943 | 39.1 | 72.7 | 1.86 | 1.57 | 1.29 |
| PR10 | 2074 | 36.5 | 67.7 | 1.85 | 1.57 | 1.28 |
| PR11 | 2108 | 34.8 | 66.2 | 1.90 | 1.60 | 1.30 |
| PR12 | 1997 | 31.9 | 56.7 | 1.78 | 1.52 | 1.26 |
| PS02 | 1829 | 41.3 | 77.5 | 1.88 | 1.58 | 1.29 |
| PS03 | 1831 | 41.4 | 77.6 | 1.87 | 1.58 | 1.29 |
| PS04 | 1827 | 41.6 | 77.9 | 1.87 | 1.58 | 1.29 |
| PS05 | 1829 | 41.2 | 78.0 | 1.89 | 1.60 | 1.30 |
| PS06 | 1817 | 41.4 | 78.3 | 1.89 | 1.59 | 1.30 |
| PS07 | 1828 | 41.1 | 77.7 | 1.89 | 1.59 | 1.30 |
| PS08 | 1846 | 41.0 | 77.3 | 1.88 | 1.59 | 1.29 |
| PS09 | 1839 | 41.1 | 77.5 | 1.89 | 1.59 | 1.30 |
| PS10 | 1838 | 40.6 | 77.0 | 1.90 | 1.60 | 1.30 |
| PM02 | 1862 | 40.1 | 73.6 | 1.83 | 1.56 | 1.28 |
| PM03 | 1885 | 38.0 | 74.6 | 1.96 | 1.64 | 1.32 |
| PM04 | 1917 | 39.5 | 74.8 | 1.89 | 1.60 | 1.30 |
| PM05 | 1900 | 40.3 | 72.3 | 1.79 | 1.53 | 1.26 |
| PM06 | 1922 | 38.4 | 71.5 | 1.86 | 1.57 | 1.29 |
| PM07 | 2086 | 38.0 | 68.7 | 1.81 | 1.54 | 1.27 |

Note: * allowable ductility has been calculated considering far field earthquake

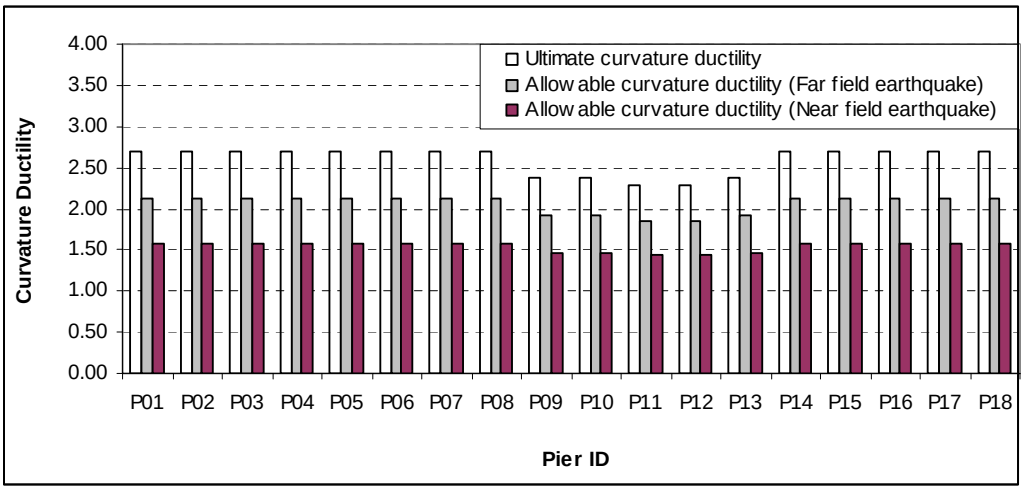


Figure 7. Ultimate and allowable curvature ductility of Khilgaon flyover piers

The ultimate curvature ductility along with allowable ductility is presented in Figure 7. It is seen from the figure that the ultimate curvature ductility is different for different piers. The differences may be due to difference in longitudinal reinforcements. The allowable curvature ductility as seen from the figure is of the order of 1.5 under near field earthquake.

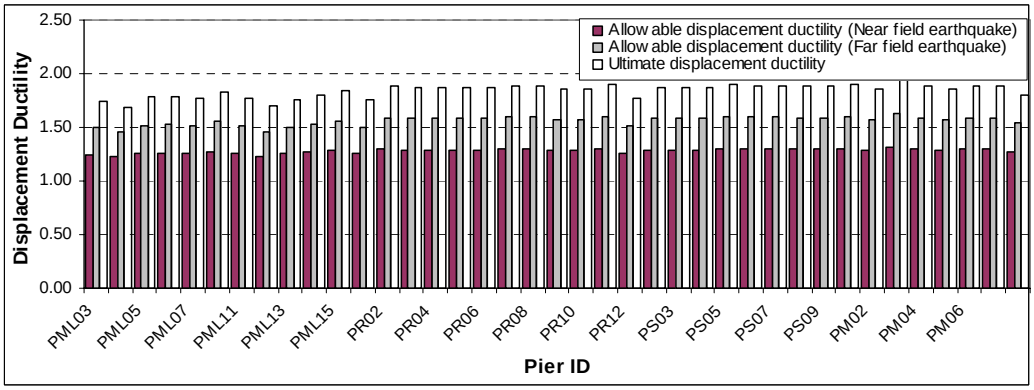


Figure 8. Ultimate and allowable displacement ductility of Khilgaon flyover piers

It is seen from Figure 8. that the allowable displacement ductility for far filed earthquake is of the order of 1.5, while that for near field earthquake is 1.3.

### 3.4 *Shear strength*

The shear strength of the piers is estimated from the code specified equations of JRA (2002) and AASHTO (2005). The shear strength of piers obtained from calculations by using the JRA and AASHTO equation are presented in Figure 9. It is seen that the shear strengths obtained from AASHTO's equation much larger than those obtained from the JRA equations. The reasons for that are due to the negligence of many factors into considerations. It is seen from the f shear strength and lateral strength of the piers are shown in Figure 9. that the shear strength of the piers of  of Rajarbagh and Saidabd arm is of the order of 1000 kN, while that of the Malibagh arm is of the order of 750 kN as calculated by using the JRA equations. Apart from the shear strength, the bending strength of the piers in terms of lateral strengths are also presented in the same figure. It can be seen that, the shear strength of the piers are much less than the bending strength of the piers. It means that a pier is supposed to fail in shear mode which brittle and hence, catastrophic.

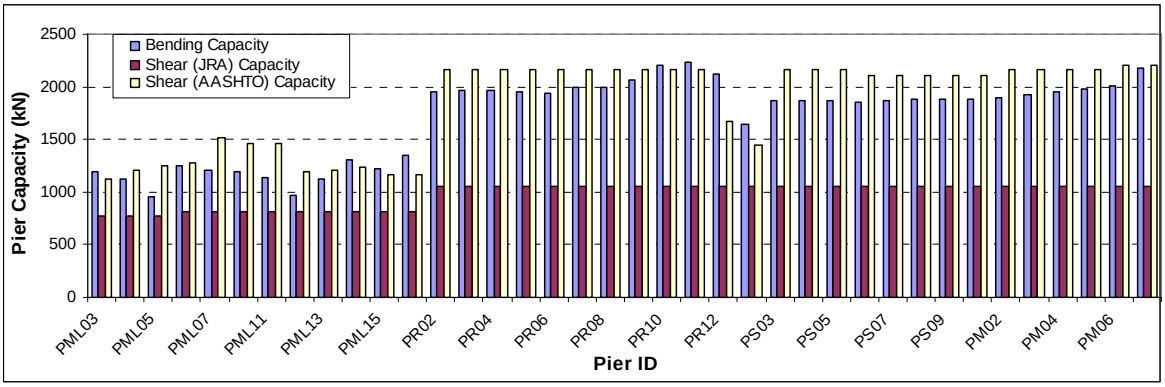


Figure 9. Bending and shear strength capacity of Khilgaon flyover piers

## 3.5 *Lateral strength*

The lateral strengths of the pier are obtained from the results of the shear strength and bending strength of the pier in horizontal direction and normalized by the respective weights from the super structures. The minimum of the bending and shear strength is taken as the lateral strength of the pier. The lateral strengths of the piers of the flyover are presented in Fig. 3.6. It is seen form the figure that the minimum lateral strength of the pier presented in Figure 10. is 0.3W.

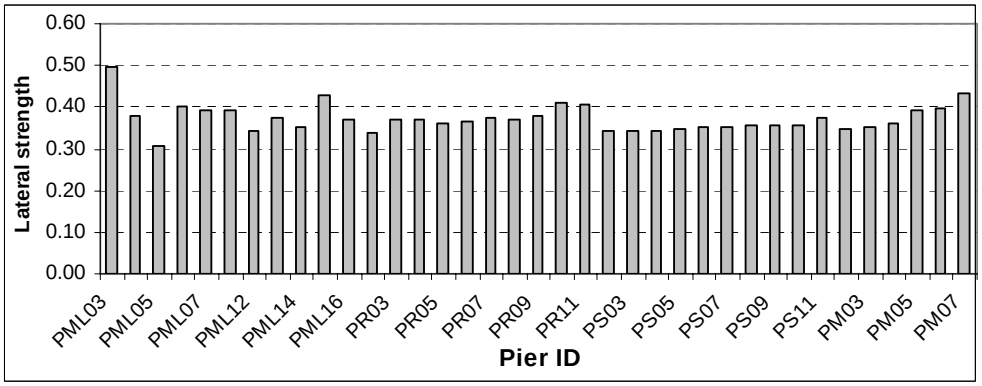


Figure 10. Lateral strength of Khilgaon flyover pier in normalized form

## 4 CONCLUSIONS

Lateral strengths of the piers of Khilgaon flyover are obtained by carrying out nonlinear analyses. Moment-curvature relationship of pier bottom sections are obtained at first step to obtain the characteristic moments: yield moment, ultimate moments, and the lateral strengths are obtained from the bending strengths and shear strengths of the piers.

The bending capacity of the piers is found larger that that of the shear capacity which predicts the shear mode of failure of the piers under a future earthquake of moderate earthquake. The normalized lateral strength of the pier is of the order of 0.3 to 0.45.

The ultimate curvature and displacement ductility as obtained from the analysis of pier are 2.7, and 1.8.

## REFERENCES

AASHTO, 2002, "LRFD Bridge Design Specifications,"_American Association of State Highway and Transportation Officials, 2nd ed., Washington, D.C., USA.

AASHTO. 1998. LRFD Bridge design specifications, Second edition, American Association of State Highway and Transportation Officials, 1998.

Ahmad, S. H. and S. P. Shah.1982. "Complete triaxial stress-strain curves of concrete." Journal of Structural Division, ASCE, 108(4), pp. 728-742.

Ali, M. H. and Choudhury, J.R. 1992. Tectonics and Earthquake Occurrence in Bangladesh, Paper presented at 36th Annual Convention of the Institution Engineers, Dhaka.

Ali, M. H. and Choudhury, J.R. 1994. Seismic Zoning of Bangladesh, Paper presented at the International Seminar on Recent Developments in Earthquake Disaster Mitigation, Institute of Engineers, Dhaka.

Caltrans. 1999. Bridge Design Specifications Manual, California Department of Transportation, Sacramento, CA., USA, 1998.
Eurocode 8. 1998. Design Provisions for earthquake resistance of structures, European Standards, Brussels, 1998.
Hoshikuma, J., Kawashima, K., Nagaya, K., Taylor, A.W. (1997). Stress-strain model for reinforced concrete in bridge piers. Journal of structural Engineering, ASCE 1997; 123(5): 624-33.
JRA. 2002. Specifications for highway bridges, Part V: Seismic Design, Japan Road Association, 2002.
JSCE. (2000). Earthquake resistant design codes in Japan, Japan Society of Civil Engineers, 2000.
Mander J. B., M. J. N. Priestley and R. Park. 1988a. "Theoretical stress–strain model for confined concrete. Journal of Structural Division, ASCE, 114(8): pp. 1804–1826.
Mander J. B., M. J. N. Priestley and R. Park. 1988b. "Observed stress-strain behavior of confined concrete." Journal of Structural Division, ASCE, 114(8): pp. 1827–1849.
Wang, P. T., Shah, S. P. and Naaman, A. E. 1987. "Stress-strain curves of normal and light weight concrete in compression." ACI Structural Journal, 75(62), pp. 603-611.